

On robustness and leadership in Markov switching consensus networks

Sarah Huiyi Cen, Vaibhav Srivastava, and Naomi Ehrich Leonard

Abstract—We examine the influence of time-varying interactions, which are modeled by a Markov switching graph (MSG), on noisy multi-agent dynamics. Our focus is on the robustness of both consensus and leader-follower tracking dynamics in the presence of stochastic noise, and we derive expressions for the steady-state covariance of the system's deviation from consensus and tracking error, respectively. We use these measures to quantify individual and group performance as functions of the interaction graphs and graph switching matrix. We extend notions of robustness and joint centrality indices for static graphs to MSGs.

I. INTRODUCTION

Many systems rely on the cooperation of agents, each performing a task and strategically arranged to collectively achieve a goal. Such multi-agent systems are ubiquitous across disciplines from biology to engineering to economics. Typically, real multi-agent systems operate in noisy environments, and the interactions among agents vary with time. For the successful design of such systems, it is imperative to understand the influences of time-varying interactions and noise on the individual as well as collective performance.

In this paper, we examine the effects of time-varying interactions among agents on the robustness of consensus dynamics and the related leader-follower collective reference tracking problem in the presence of stochastic noise. We model the time-varying interactions with a Markov switching graph (MSG), defined by a set of static graphs and a Markov chain that describes the transitions among these graphs.

The robustness of consensus problem for static interaction graphs [1]–[5] has received significant attention. Extending these results to time-varying graphs (TVG) is challenging due to the limited analytic tractability of time-varying dynamical systems. Consensus dynamics have been studied for deterministically time-varying graphs [6], [7] and stochastically time-varying graphs [8]–[10], but these analyses are not applicable in the presence of noise. For example, a contraction analysis-based approach cannot be immediately applied in the presence of stochastic forcing terms. We leverage the structure of MSGs, a special class of stochastically time-varying graphs, to understand the robustness properties of noisy consensus dynamics. The consensus dynamics under

MSGs have been studied in [8], but to the best of our knowledge, the influence of noise on the performance of consensus in MSGs has not been explored.

In the noisy leader-follower collective reference tracking problem, a set of cooperating agents track a reference signal despite signal and communication noises. A subset of these agents, the leaders, have access to the external signal while the rest, the followers, rely solely on information communicated from their neighbors. This framework has received attention in the context of the optimal leader selection problem, i.e., the designation of a leader set that optimizes the group performance [11]–[14]. Leader selection problems have been studied for TVGs that transition much more slowly than the consensus dynamics and for stochastic TVGs resulting from random link failure [14]. We investigate the noisy leader-follower collective reference tracking problem for MSGs. Our approach does not require the time-scale separation between graph and consensus dynamics, and it accounts for more general stochastic TVGs than in [14].

Our results leverage the theory of continuous-time Markov jump linear systems (CT MJLS) [15] to characterize the robustness and leadership properties in time-varying multi-agent networks. Our main contributions are three-fold. First, we derive measures of system performance for the noisy consensus and noisy leader-follower reference tracking problems as functions of the graph structures and graph switching matrix defining the MSG. Second, we show how these measures can be used to extend notions of robustness and centrality measures for static graphs to MSGs. Third, we illustrate how system performance varies and often improves for the dynamic graph as compared to the static graph.

In Sections II and III, we introduce the two noisy coordination problems for MSGs and review key concepts for the CT MJLS, respectively. In Section IV, we rigorously analyze performance under the two coordination problems. In Section V, we present notions of robustness and centrality measures for MSGs. We numerically illustrate our results in Section VI and conclude in Section VII.

II. TWO NOISY DISTRIBUTED COORDINATION PROBLEMS UNDER MARKOV SWITCHING GRAPHS

Consider a system comprising a switching network of m agents with system state $\mathbf{x}(t) \in \mathbb{R}^m$, where $x_i(t)$ is the state of agent i at time $t \geq 0$. Each agent i sends and receives information from its set of neighbors $N_i(t)$. The resulting communication topologies make up the undirected, unweighted time-varying graph $\mathcal{G}(t) = (\mathcal{V}, \mathcal{E}(t), Y(t))$ for the set of nodes $\mathcal{V} = \{1, \dots, m\}$, set of edges $\mathcal{E}(t) \subseteq \mathcal{V} \times \mathcal{V}$, and adjacency matrix $Y(t) \in \mathbb{R}^{m \times m}$. Each graph node

This research has been supported by ONR grant N00014-14-1-0635 and ARD grant W911NF-14-1-0431

S. H. Cen is with the Department of Engineering Science, University of Oxford, Oxford, OX1 3PJ, UK (email: sarah@robots.ox.ac.uk).

V. Srivastava is with the Department of Electrical and Computer Engineering, Michigan State University, East Lansing, MI 48824, USA (email: vaibhav@egr.msu.edu).

N. E. Leonard is with the Department of Mechanical and Aerospace Engineering, Princeton University, Princeton, NJ 08544, USA (e-mail: naomi@princeton.edu).

corresponds to an agent in the network, which contains an edge (i, j) between nodes i and j at time t if $j \in N_i(t)$. $Y_{ij}(t) = 1$ if edge (i, j) exists at time t and $Y_{ij}(t) = 0$, otherwise. Since $\mathcal{G}(t)$ is undirected, (i, j) implies (j, i) , and Y is symmetric. The degree of node i at time t is $d_i(t) = \sum_{j=1}^m Y_{ij}(t)$, and $D(t) = \text{diag}(d_1(t), d_2(t), \dots, d_m(t))$. The Laplacian matrix of $\mathcal{G}(t)$ at time t is $L(t) = D(t) - Y(t)$.

We first consider the *noisy consensus* problem wherein a set of agents, each with its own opinion x_i , attempts to achieve agreement. Specifically, this analysis studies the network consensus problem [7] under stochastic noise for TVGs. The continuous-time dynamics are

$$d\mathbf{x}(t) = -L(t)\mathbf{x}(t)dt + Fd\mathbf{W}(t), \quad (1)$$

where F is the system noise matrix and $d\mathbf{W}(t)$ is the m -dimensional standard Wiener process increment. Consensus is achieved when $\mathbf{x} = \alpha \mathbf{1}_m$, where $\alpha \in \mathbb{R}$ is the agreement value and $\mathbf{1}_m$ is the $m \times 1$ vector of all 1's.

Next, we consider the *noisy leader-follower reference tracking* problem, in which the agents seek to track an external reference signal $\theta \in \mathbb{R}$ such that x_i represents agent i 's tracking estimate of θ . A subset of agents, called *leaders*, directly measure θ , which is affected by noise, and the remaining agents, called *followers*, do not directly measure θ . All agents exchange information via noisy communication with their neighbors. The continuous-time dynamics are

$$d\mathbf{x}(t) = -(L(t)\mathbf{x}(t) + K(\mathbf{x}(t) - \theta \mathbf{1}_m))dt + Fd\mathbf{W}(t), \quad (2)$$

where the leadership matrix $K \in \mathbb{R}^{m \times m}$ is a diagonal matrix with entries $\{\kappa_1, \kappa_2, \dots, \kappa_m\}$. If agent i is a leader, then $\kappa_i = \kappa > 0$ such that all leaders share the same gain κ . If agent i is a follower, then $\kappa_i = 0$. The cardinality of the leader set \mathcal{K} is given by $|\mathcal{K}|$. Without loss of generality, we let $\theta = 0$, reducing the dynamics (2) to

$$d\mathbf{x}(t) = -M(t)\mathbf{x}(t)dt + Fd\mathbf{W}(t), \quad (3)$$

where $M(t) = L(t) + K$.

We assess network performance using the following definitions of node and system errors, which apply only to systems for which the steady-state covariance exists. Define the *node error* E_i of node i as the steady-state variance of x_i :

$$E_i(\Sigma_{ss}(\mathbf{x})) = (\Sigma_{ss}(\mathbf{x}))_{ii},$$

where $\Sigma_{ss}(\mathbf{x})$ is the steady-state covariance of \mathbf{x} . Define the *system error* E as the steady-state variance of \mathbf{x} :

$$E(\Sigma_{ss}(\mathbf{x})) = \text{tr}(\Sigma_{ss}(\mathbf{x})) = \sum_{i=1}^m E_i(\Sigma_{ss}(\mathbf{x})).$$

We study the two coordination problems (1) and (3) under the assumption that the system switches between a finite set of static interaction graphs $\mathbb{G} = \{G_1, \dots, G_n\}$ according to a Markov chain (MC), where $G_i = (\mathcal{V}, \mathcal{E}_i, \mathcal{Y}_i)$. The resulting TVG is known as a *Markov switching graph* (MSG). Under a given MSG \mathcal{G} , the linear dynamical systems (1) and (3) are known as *Markov jump linear systems* (MJLS) [16]. Recall that the total number of possible unweighted graphs

for a given finite node set is also finite. Hence, the set \mathbb{G} is assumed to be finite without loss of generality. Let $S = \{1, \dots, n\}$ be the graph index set.

Let the graph switching behavior in (1) and (3) be governed by a continuous-time MC (CTMC). For the graph set \mathbb{G} , the CTMC is specified by the infinitesimal time-homogeneous generator matrix $\Gamma \in \mathbb{R}^{n \times n}$ with elements:

$$\Gamma_{ij} = \begin{cases} q_{ij}, & i \neq j, \\ -v_i, & i = j, \end{cases}$$

for $i, j \in S$. Here, $v_i = \sum_{j \in S \setminus i} q_{ij}$ is the holding rate of graph G_i , and $q_{ij} \geq 0$ is the transition rate from G_i to G_j . Intuitively, q_{ij} is the rate parameter of an exponential distribution that determines the probability that the system in graph G_i transitions to graph G_j with time [15]. All rows in Γ sum to 0, and $-\Gamma$ is a Laplacian matrix.

Let Δ_n be the $(n - 1)$ -dimensional probability simplex in \mathbb{R}^n . Then, for the CTMC with the generator matrix Γ , $\pi(t) \in \Delta_n$ is the probability distribution over \mathbb{G} at time t . Specifically, $\pi_i(t)$ is the probability that $\mathcal{G}(t) = G_i$, and $\sum_{i=1}^n \pi_i(t) = 1$. From [15], $\pi(t) = e^{\Gamma^\top t} \pi(0)$.

We study the two coordination problems under the following assumptions for the MSG:

Assumption 1: The underlying CTMC is *ergodic*. \square

Assumption 2: Every graph in the set \mathbb{G} is unweighted, undirected, and connected. \square

Under Assumption 1, the CTMC has a unique stationary distribution π_{ss} such that $\lim_{t \rightarrow \infty} \pi(t) = \pi_{ss}$. Ergodicity implies that Γ^\top has exactly one eigenvalue at 0 with the right eigenvector π_{ss} (i.e., $\pi_{ss} = e^{\Gamma^\top} \pi_{ss}$) and all others in the left half-plane. Assumption 2 can be relaxed under certain conditions, but for clarity of exposition, we keep it.

III. PRELIMINARIES ON MARKOV JUMP LINEAR SYSTEMS

Consider the following CT MJLS:

$$d\mathbf{x}(t) = -Z(t)\mathbf{x}(t)dt + Fd\mathbf{W}(t), \quad (4)$$

where $Z(t) \in \mathbb{R}^{m \times m}$ corresponds to the network graph at time t of the MSG with generator matrix Γ . Let $Z(t) = Z_i$ whenever $\mathcal{G}(t) = G_i$. We now solve for the dynamics of the mean and second moment of $\mathbf{x}(t)$ evolving according to (4).

For the following proposition, let $\boldsymbol{\mu}(t) = \mathbb{E}[\mathbf{x}(t)]$ represent the mean. The contribution of graph $G_i \in \mathbb{G}$ to the mean is $\boldsymbol{\mu}^i(t) = \mathbb{E}[\mathbf{x}(t)\mathcal{I}(\mathcal{G}(t) = G_i)]$ such that $\boldsymbol{\mu}(t) = \sum_{i=1}^n \boldsymbol{\mu}^i(t)$, where $\mathcal{I}(\cdot)$ is the indicator function. Vertically stacking the means for all graphs gives the vector:

$$\boldsymbol{\nu}(t) = [\boldsymbol{\mu}^1(t)^\top, \boldsymbol{\mu}^2(t)^\top, \dots, \boldsymbol{\mu}^n(t)^\top]^\top.$$

Similarly, let the second moment $C(t) = \mathbb{E}[\mathbf{x}(t)\mathbf{x}(t)^\top]$. The contribution of graph $G_i \in \mathbb{G}$ to the second moment is $C^i(t) = \mathbb{E}[\mathbf{x}(t)\mathbf{x}(t)^\top \mathcal{I}(\mathcal{G}(t) = G_i)]$ such that $C(t) = \sum_{i=1}^n C^i(t)$. Vertically stacking the vectorized second moments for all graphs gives the vector:

$$\mathbf{c}(t) = [\mathbf{c}^1(t)^\top, \mathbf{c}^2(t)^\top, \dots, \mathbf{c}^n(t)^\top]^\top,$$

where $\mathbf{c}^i(t) = \text{vec}(C^i(t))$ and $\text{vec}(\cdot)$ is the vectorization operator. For the remaining analysis, let $Q = FF^\top$, $\mathcal{N} =$

$\text{diag}_n(Z_i) - \Gamma^T \otimes \mathbb{I}_m$, and $\mathcal{M} = \text{diag}_n(Z_i \oplus Z_i) - \Gamma^T \otimes \mathbb{I}_{m^2}$, where \otimes and \oplus are the Kronecker product and sum operators, respectively, and $\text{diag}_n(A_i)$ is the block-diagonal matrix with entries $\{A_1, A_2, \dots, A_n\}$.

Proposition 1: The following statements hold for the CT MJLS (4) with an MSG satisfying Assumptions 1 and 2:

- (i) The dynamics of the mean term $\nu(t)$ are

$$\dot{\nu}(t) = -\mathcal{N}\nu(t); \quad (5)$$

- (ii) The dynamics of the second moment term $c(t)$ are

$$\dot{c}(t) = -\mathcal{M}c(t) + \pi(t) \otimes \text{vec}(Q). \quad (6)$$

Proof: This result is standard in MJLS literature. See, for example, [16], [17, Proposition 3.5]. ■

IV. PERFORMANCE OF DISTRIBUTED COORDINATION UNDER MARKOV SWITCHING GRAPHS

In this section, we study and interpret the performance of the two noisy coordination problems described in Section II under MSGs. Let $\mathbf{h}_{S,1} = \text{vec}(\mathbb{I}_{m^2})^\top$ and $\mathbf{h}_{S,n} = \mathbf{1}_n^\top \otimes \mathbf{h}_{S,1}$. Furthermore, let $\mathbf{h}_{N,1}^i = \text{vec}(\mathbb{O}_{m^2}^i)^\top$ and $\mathbf{h}_{N,n}^i = \mathbf{1}_n^\top \otimes \mathbf{h}_{N,1}^i$, where $\mathbb{O}_{m^2}^i$ is the $m^2 \times m^2$ matrix containing all zeros except at element (i, i) , which takes the value 1. Then, $\mathbf{h}_{S,n}c$ is the trace of second moment $\mathbb{E}[\mathbf{x}\mathbf{x}^\top]$, and $\mathbf{h}_{N,n}^i c$ is its diagonal element (i, i) corresponding to node i . At steady state, these expressions are the contributions of the second moment to the system and node errors, respectively.

A. Noisy consensus under MSGs

Let \mathcal{N}_c and \mathcal{M}_c be the system matrices in (5) and (6) after specializing Proposition 1 to the CT MJLS (1).

Lemma 1: For the noisy consensus dynamics (1), under Assumptions 1 and 2, both \mathcal{N}_c and \mathcal{M}_c have exactly one eigenvalue at 0 each; all others lie in the right half-plane.

Proof: When specializing Proposition 1 to (1), $Z_i = L_i$, and (4) reduces to (1). Consequently, $\mathcal{N}_c = \text{diag}_n(L_i) - \Gamma^\top \otimes \mathbb{I}_m$ and $\mathcal{M}_c = \text{diag}_n(L_i \oplus L_i) - \Gamma^\top \otimes \mathbb{I}_{m^2}$. We seek to show that \mathcal{N}_c^\top and \mathcal{M}_c^\top are effectively the Laplacian matrices of two large connected graphs that contain nm and nm^2 nodes, respectively, and each has exactly one eigenvalue at 0.

For \mathcal{N}_c^\top , $\text{diag}_n(L_i)$ is the Laplacian of a disconnected graph with n clusters, each of which is a connected subgraph of m nodes, as required. Therefore, the null space of $\text{diag}_n(L_i)$ is spanned by vectors of the form $\mathbf{a} \otimes \mathbf{1}_m$ for any $\mathbf{a} \in \mathbb{R}^n$. Because Γ describes an ergodic CTMC, $-\Gamma \otimes \mathbb{I}_m$ is the Laplacian of a connected graph, and the null space of $-\Gamma \otimes \mathbb{I}_m$ is spanned by vectors of the form $\mathbf{1}_n \otimes \mathbf{b}$ for any $\mathbf{b} \in \mathbb{R}^m$. The sum of two Laplacians is also a Laplacian. Furthermore, by Lemma 3.5 in [8], for two Laplacian matrices A and B , $\text{Null}(A+B) = \text{Null}(A) \cap \text{Null}(B)$. Therefore, $\text{Null}(\mathcal{N}_c^\top)$ is the intersection of the space spanned by $\mathbf{a} \otimes \mathbf{1}_m$ and $\mathbf{1}_n \otimes \mathbf{b}$, which is the space spanned by $\mathbf{1}_{nm}$. Since the eigenvalues of a Laplacian are either at 0 or lie strictly in the right half-plane [18] and the nullity of \mathcal{N}_c^\top is 1, the transpose \mathcal{N}_c , which shares its eigenvalues, has exactly one eigenvalue at 0. It can be verified that the corresponding right eigenvector is $\pi_{ss} \otimes \mathbf{1}_m$.

Similarly, it can be shown that \mathcal{M}_c has the unique right eigenvector $\pi_{ss} \otimes \mathbf{1}_{m^2}$ corresponding to the eigenvalue 0. ■

Due to the eigenvalues of \mathcal{N}_c and \mathcal{M}_c at 0, the second moment of \mathbf{x} in (1) diverges. However, the diverging part corresponds to the fully correlated component of agents' states and therefore does not contribute to the deviation from consensus. Borrowing terminology from [19], we label the subspace of \mathbb{R}^m spanned by $\mathbf{1}_m$ the *consensus subspace* and its orthogonal complement the *disagreement subspace*. We show that as with the static graph [1], the second moment of \mathbf{x} in (1) projected onto the disagreement subspace achieves a bounded steady-state value and measures the distance from consensus for the calculation of the system and node errors.

For the following propositions, let $\mathbf{x}^\perp \in \mathbb{R}^{m-1}$ represent the orthogonal projection of \mathbf{x} onto the $(m-1)$ -dimensional disagreement subspace $\mathbf{1}_m^\perp$. We pick $V \in \mathbb{R}^{(m-1) \times m}$ such that its rows form the orthonormal basis of $\mathbf{1}_m^\perp$ and let $\mathbb{V} = V^\top V = \mathbb{I} - \frac{1}{m} \mathbf{1}_m \mathbf{1}_m^\top$. Then, as in [1], let $\mathbf{x}^\perp = V\mathbf{x}$ and $\bar{\mathbf{x}} = V^\top \mathbf{x}^\perp$ such that $\mathbf{x} = \frac{1}{m} \mathbf{1}_m \mathbf{1}_m^\top \mathbf{x} + \bar{\mathbf{x}}$. The vector $\bar{\mathbf{x}} \in \mathbb{R}^m$ is the component of \mathbf{x} orthogonal to the consensus subspace; we refer to it as the disagreement vector. Note that $\mathbf{1}_m$ is the right eigenvector of $L(t)$ associated with the eigenvalue 0.

From (1), the disagreement dynamics are

$$d\bar{\mathbf{x}}(t) = -L(t)\bar{\mathbf{x}}(t)dt + \mathbb{V}F d\mathbf{W}(t). \quad (7)$$

Mimicking the notation in Section III, let $\bar{\boldsymbol{\mu}}(t) = \mathbb{E}[\bar{\mathbf{x}}(t)]$, $\bar{\boldsymbol{\mu}}^i(t) = \mathbb{E}[\bar{\mathbf{x}}(t)\mathcal{I}(\mathcal{G}(t) = G_i)]$ for each $i \in S$, and $\bar{\boldsymbol{\nu}}(t) = [\bar{\boldsymbol{\mu}}^1(t)^\top, \dots, \bar{\boldsymbol{\mu}}^n(t)^\top]^\top$. Let $\bar{C}(t)$, $\bar{C}^i(t)$ and $\bar{c}(t)$, the second moment terms of $\bar{\mathbf{x}}$, be defined analogously.

Proposition 2: For the disagreement dynamics (7), under Assumptions 1 and 2, the following statements hold:

- (i) the steady-state mean disagreement vector is zero, i.e.,

$$\bar{\boldsymbol{\nu}}_{ss} = \mathbf{0}_{nm}, \quad (8)$$

where $\mathbf{0}_{nm}$ is the $nm \times 1$ vector of all zeros;

- (ii) the steady-state second moment of the disagreement vector is

$$\bar{c}_{ss} = \mathcal{M}_c^+(\pi_{ss} \otimes \text{vec}(\mathbb{V}Q\mathbb{V})), \quad (9)$$

where $\mathcal{M}_c = \text{diag}_n(L_i \oplus L_i) - \Gamma^\top \otimes \mathbb{I}_{m^2}$, and \mathcal{M}_c^+ is its pseudoinverse.

Proof: Recall that $\bar{\mathbf{x}} = \mathbb{V}\mathbf{x}$. Therefore, $\bar{\boldsymbol{\mu}}^i = \mathbb{V}\boldsymbol{\mu}^i$ and $\bar{c}^i = (\mathbb{V} \otimes \mathbb{V})c^i$. Specializing Proposition 1(i) to (7) gives $\dot{\bar{\boldsymbol{\nu}}}(t) = -\mathcal{N}_c \bar{\boldsymbol{\nu}}(t)$. Then, from the proof for Lemma 1, \mathcal{N}_c has exactly one eigenvalue at 0 with the eigenvector $\pi_{ss} \otimes \mathbf{1}_m$ and all others in the right half-plane. Now, recall that $\bar{\mathbf{x}} = (\mathbb{I}_m - \frac{1}{m} \mathbf{1}_m \mathbf{1}_m^\top)\mathbf{x}$. Since any component of \mathbf{x} along the direction $\mathbf{1}_m$ is removed to get $\bar{\mathbf{x}}$, by its definition, $\bar{\boldsymbol{\nu}}$ has no component along $\pi_{ss} \otimes \mathbf{1}_m$ with two consequences. First, the eigenvalue at 0 is irrelevant, and $\bar{\boldsymbol{\nu}}$ has a steady-state solution. Second, as all other eigenvalues lie strictly in the right half-plane, the steady-state solution must be $\bar{\boldsymbol{\nu}}_{ss} = \mathbf{0}_{nm}$.

Similarly, specializing Proposition 1(ii) to (7) gives $\dot{\bar{c}}(t) = -\mathcal{M}_c \bar{c}(t) + \pi(t) \otimes \text{vec}(\mathbb{V}Q\mathbb{V})$. It can be shown analogously to \mathcal{N}_c that \mathcal{M}_c has exactly one eigenvalue at 0 with the eigenvector $\pi_{ss} \otimes \mathbf{1}_{m^2}$ that is unrelated to the evolution of

c. It can also be shown that all other eigenvalues of \mathcal{M}_c lie strictly in the right half-plane, meaning that $\bar{\mathbf{c}}(t)$ has a steady-state solution. At steady state, $\dot{\bar{\mathbf{c}}}_{ss} = \mathbf{0}_{nm^2}$ and $\pi(t) = \pi_{ss}$, from which we solve for $\bar{\mathbf{c}}_{ss}$. ■

This result implies that the steady-state second moment of the disagreement vector is in fact the steady-state covariance. That is, the system and i -th node errors of (1) computed on the disagreement space are $\mathbf{h}_{S,n}\bar{\mathbf{c}}_{ss}$ and $\mathbf{h}_{N,n}^i\bar{\mathbf{c}}_{ss}$, respectively.

B. Noisy leader-follower reference tracking under MSGs

Let \mathcal{N}_k and \mathcal{M}_k be the system matrices in (5) and (6) after specializing Proposition 1 to the CT MJLS (3).

Lemma 2: For the noisy leader-follower reference tracking dynamics (3), under Assumptions 1 and 2, all eigenvalues of matrices \mathcal{N}_k and \mathcal{M}_k lie strictly in the right half-plane.

Proof: When specializing Proposition 1 to the CT MJLS (3), $Z_i = L_i + K = M_i$, and (4) reduces to (3). Consequently, $\mathcal{N}_k = \text{diag}_n(M_i) - \Gamma^\top \otimes \mathbb{I}_m$ and $\mathcal{M}_k = \text{diag}_n(M_i \oplus M_i) - \Gamma^\top \otimes \mathbb{I}_{m^2}$. It follows that $\mathcal{N}_k = \mathcal{N}_c + I_n \otimes K$. From Lemma 1, \mathcal{N}_c^\top is a Laplacian matrix with the one-dimensional null space $\mathbf{1}_{nm}$. Thus, \mathcal{N}_k is a diagonal perturbation of \mathcal{N}_c and has all eigenvalues strictly in the right half-plane as long as $|\mathcal{K}| > 0$. Analogously, all eigenvalues of \mathcal{M}_k also lie strictly in the right half-plane. ■

Thus, in contrast to the noisy consensus problem, the noisy leader-follower reference tracking problem does not require the separation of consensus and disagreement subspaces since the presence of leaders removes the eigenvalue at 0 from \mathcal{N}_k and \mathcal{M}_k . For the following proposition, let the specialization of $\nu(t)$ and $\mathbf{c}(t)$ in (5) and (6) to the CT MJLS (3) be $\hat{\nu}(t)$ and $\hat{\mathbf{c}}(t)$, respectively.

Proposition 3: For the leader-follower reference tracking dynamics (3) with $|\mathcal{K}| > 0$ and under Assumptions 1 and 2, the following statements hold:

- (i) the steady-state mean of the state vector is zero, i.e.,

$$\hat{\nu}_{ss} = \mathbf{0}_{nm}; \quad (10)$$

- (ii) the steady-state second moment of the state vector is

$$\hat{\mathbf{c}}_{ss} = \mathcal{M}_k^{-1}(\pi_{ss} \otimes \text{vec}(Q)), \quad (11)$$

where $\mathcal{M}_k = \text{diag}_n(M_i \oplus M_i) - \Gamma^\top \otimes \mathbb{I}_{m^2}$.

Proof: For the CT MJLS (3), all eigenvalues of \mathcal{N}_k lie strictly in the right half-plane, meaning that $\hat{\nu}(t)$ has a steady-state solution. Since $\dot{\hat{\nu}}(t) = \mathcal{N}_k\hat{\nu}(t)$ from Proposition 1 and $\hat{\nu}(t) = \mathbf{0}_{nm}$ at steady state, it must be true that $\hat{\nu}_{ss} = \mathbf{0}_{nm}$. Similarly, since the eigenvalues of \mathcal{M}_k also lie strictly in the right half-plane, there exists a steady-state solution for $\hat{\mathbf{c}}(t)$. At steady state, $\dot{\hat{\mathbf{c}}}(t) = \mathbf{0}_{nm^2}$ and $\pi(t) = \pi_{ss}$, from which we solve for $\hat{\mathbf{c}}_{ss}$. ■

As in Section IV-A, only the steady-state second moment is needed to determine the system and i -th node errors of (3), which are given by $\mathbf{h}_{S,n}\hat{\mathbf{c}}_{ss}$ and $\mathbf{h}_{N,n}^i\hat{\mathbf{c}}_{ss}$, respectively.

Equations (9) and (11) express the relationship between performance and graph design. Understanding these results would reveal how the graph topologies and switching behavior, which are encoded in \mathcal{M} , affect the MSG's ability

to propagate information. However, unlike π_{ss} and Q , the influence of \mathcal{M} on the error is difficult to interpret due to the inverse matrices in (9) and (11). Intuitively, these matrices contain the most information since it is the inverse operation that performs the mixing of graphs in \mathbb{G} according to Γ .

V. ROBUSTNESS AND LEADERSHIP INDICES FOR MSGs

The robustness of a system is measured by its deviation from the desired result. For consensus, this deviation is isolated by projecting the system state onto the disagreement subspace. Proposition 2 shows that for noisy consensus under MSGs, this disagreement state is a stochastic process that, in the limit $t \rightarrow +\infty$, has zero mean and finite covariance. The component of covariance in consensus subspace is completely correlated (i.e. spanned by $\mathbf{1}_m\mathbf{1}_m^\top$) and thus disregarded because it does not contribute to the deviation from consensus. For the leader-follower reference tracking problem, robustness indicates the system's ability to track the external signal in the presence of noise through the deviation of the agents' tracking estimates from the true reference value. Given a leader set \mathcal{K} , this robustness reflects the ability of \mathcal{K} to drive all agents' tracking estimates to θ .

As discussed in [1], the trace of the steady-state covariance (i.e. the system error) measures the mean squared distance of the system state from consensus and, for a static undirected graph, corresponds to the \mathcal{H}_2 norm of (7) [20], [21]. The system error of (7) under a static graph has been related to graph resistance (see [21], [22] for directed graphs) and is widely used to quantify the robustness of consensus. In a similar spirit, we propose a new notion of *robustness of consensus for MSGs* defined by $1/(\mathbf{h}_{S,n}\bar{\mathbf{c}}_{ss})$ and call it the *system robustness index*. Similarly to [23], this can be used to rank, design, or dynamically rearrange MSG topologies for better performance. We also introduce the *node robustness index for MSGs* defined by $1/(\mathbf{h}_{N,n}^i\bar{\mathbf{c}}_{ss})$ for node i .

In the case that agents in the network measure an external stimulus, the variance of an agent's state \bar{x}_i about the correct decision reflects its decision-making accuracy [24] and figures critically in its speed-accuracy trade-off [25]. Accordingly, the inverse of the steady-state variance of \bar{x}_i is called the node certainty index in [24], which showed that, for a static graph, this index is a monotone function of the node's information centrality [26].

For noisy leader-follower reference tracking, the system error is the mean squared tracking error over all agents. The tracking performance is largely dictated by the leader nodes, and the leader selection problem has consequently received significant attention for static noisy consensus networks [11]–[14], [27]. For the static graph, [13] shows, firstly, that under the constraint $|\mathcal{K}| = 1$, the most information-central node minimizes the system error when assigned as the leader and, secondly, that the system error also leads to the notion of joint centrality for the optimal selection of \mathcal{K} for $|\mathcal{K}| > 1$ and this depends on network resistances. Other centrality measures are derived from system error for static consensus networks in [28]. In a similar spirit, we define *joint robustness centrality index of a set of nodes \mathcal{K} in MSGs* as

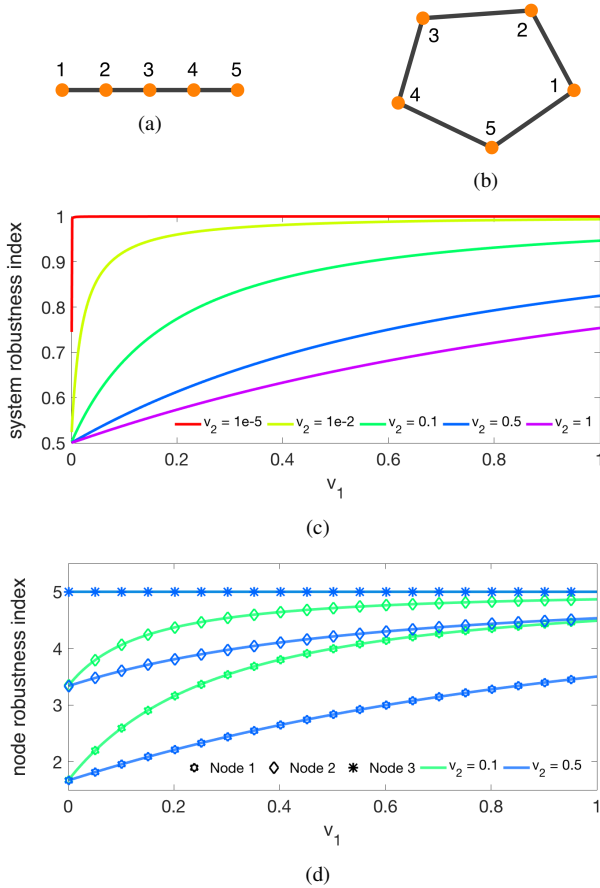


Fig. 1: Noisy consensus dynamics (1) under the MSG with state space comprising a line graph G_1 shown in panel (a) and a ring graph G_2 shown in panel (b) and defined by the parametrized generator matrix (12). For a fixed $\epsilon = 0.5$, panels (c) and (d) chart the system and node robustness indices, respectively, across a range of $v_1 = q_{12}$ and $v_2 = q_{21}$ values.

the inverse of the system error for (3) with the leader set \mathcal{K} and $\kappa \rightarrow +\infty$, i.e., $\lim_{\kappa \rightarrow +\infty} 1/(\mathbf{h}_{S,n} \hat{\mathbf{c}}_{ss})$. The optimal leader set of (3) maximizes this quantity.

VI. NUMERICAL ILLUSTRATIONS

In this section, we illustrate our results through the simulations of simple MSGs. Let the agents be independently affected by noise of the same intensity such that $F = \mathbb{I}$.

First, we examine the noisy consensus dynamics (1) under MSGs with the state space $\mathbb{G} = \{G_1, G_2\}$ comprising the line and ring graphs in Figs. 1(a)-(b) and the generator matrix

$$\Gamma = \epsilon \begin{bmatrix} -q_{12} & q_{12} \\ q_{21} & -q_{21} \end{bmatrix}, \quad (12)$$

where $q_{ij} = v_i$. Recall that Γ 's off-diagonal elements q_{ij} scale with the MSG's propensity to switch from G_i to G_j . Accordingly, ϵ controls the network's overall rate of graph switching. We fix $\epsilon = 0.5$ and study the system and node robustness indices as functions of $q_{12} = v_1$ and $q_{21} = v_2$ in Fig. 1(c)-(d). Fig. 1 illustrates that, in general, the MSG benefits from spending more time in the more connected topology. In this case, the performance improves when the MSG lingers in the ring topology (low q_{21}) and/or

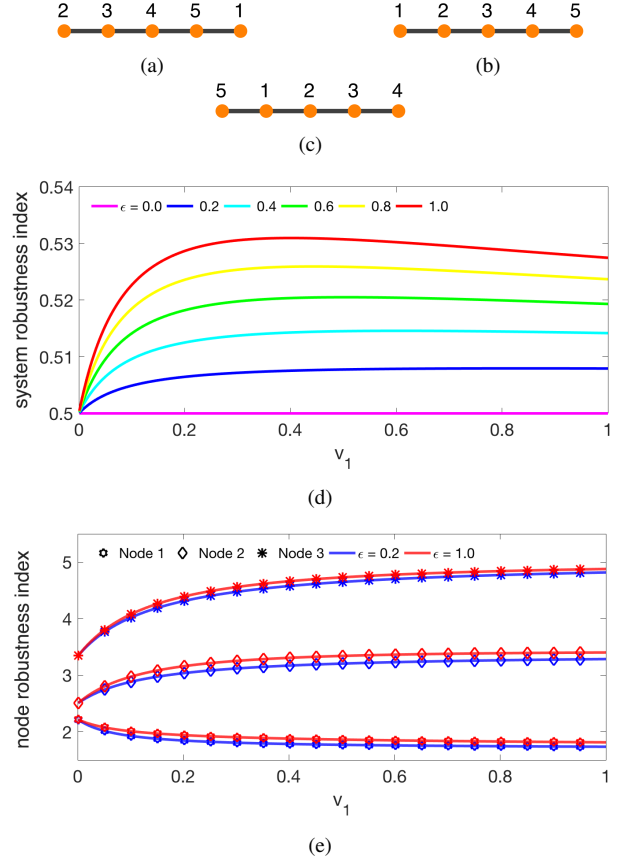


Fig. 2: Noisy consensus dynamics (1) under the MSG with state space comprising G_1, G_2 and G_3 shown in panels (a), (b), and (c), respectively, and defined by the parametrized generator matrix (13) with $v_2 = 0.1$. Panels (d) and (e) chart the system and node robustness indices, respectively, across a range of v_1 and ϵ values.

transitions to the ring more frequently (high q_{12}). Fig. 1(c) also suggests that if q_{12} is sufficiently high compared to q_{21} , the performance only improves marginally for rising q_{12} , which reveals that lengthening the time the system spends as a ring has diminishing returns. Fig. 1(d) demonstrates that the nodes do not benefit equally from the addition of edge (1, 5). In addition, the robustness curve of node 3 shows that, for this MSG, only the shortest paths between nodes affect success as node 3 does not benefit from additional longer routes to previously accessible nodes (e.g. the extra path 3-4-5-1 in the ring does not improve node 3's robustness since the shorter path 3-2-1 already exists in the line).

Second, we investigate the noisy consensus dynamics (1) under \mathbb{G} comprising graphs G_1, G_2, G_3 , shown in Figs. 2(a), (b), (c), respectively, and the generator matrix

$$\Gamma = \epsilon \begin{bmatrix} -q_{12} & q_{12} & 0 \\ q_{2j} & -2q_{2j} & q_{2j} \\ 0 & q_{32} & -q_{32} \end{bmatrix}, \quad (13)$$

where we set $q_{12} = q_{32}$ and $v_2 = 2q_{2j} = 0.1$. This system cannot transition directly between G_1 and G_3 . Unlike in the previous case, this MSG comprises three equally connected topologies that would individually produce identical system

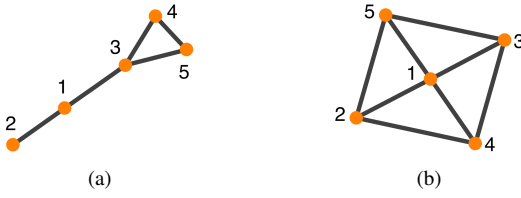


Fig. 3: Two topologies of a five-node MSG.

errors. We illustrate the system and node robustness indices as functions of $v_1 = q_{12}$ and ϵ in Figs. 2(d)-(e). The system robustness curves in Fig. 2(d) are concave and contain finite non-zero global maxima, which indicates that, unlike in the simpler line-ring case, the optimal MSG prefers to switch between graphs in order to balance the information flow across the nodes. Fig. 2(e) shows three revealing facts. First, some nodes gain from increasing q_{12} while others worsen, which causes the maxima in system robustness. Second, node 3 clearly does best with increasing q_{12} . Interestingly, node 2 also benefits from spending more time in G_2 despite its central placement in G_3 , suggesting that obtaining a highly central position is less crucial than avoiding the least central ones. Finally, as ϵ increases, the robustness indices rise, meaning that, for the same stationary distribution, performance improves when switching occurs more often.

Lastly, we study the noisy leader-follower reference tracking problem (3) in the case of a single leader. Consider the MSG comprising the two graphs in Fig. 3 and defined by the generator matrix (12) with $q_{12} = q_{21} = 1$. Then, for $\kappa = +\infty$, any $\epsilon > 0$, and $|K| = 1$, the nodes listed in order of decreasing robustness centrality index (i.e. leader potential) are 1-3-4-5-2. Interestingly, this is the same as the list of nodes in order of decreasing node robustness index for the noisy consensus problem (1) under the same MSG when $\epsilon = 10$, but it differs for $\epsilon = 1$, in which case, the ordered list by decreasing node robustness index is 3-1-4-5-2.

VII. CONCLUSION AND FUTURE WORK

In this paper, we examined the noisy distributed consensus and noisy leader-follower reference tracking problems under Markov switching graphs. We derived measures for the robustness of consensus and the joint robustness centrality of a leader set for MSGs. Through examples, we gained insights into the effects of the network's structure and switching behavior on system performance. Two compelling branches of future work are the decoding and characterizing of \mathcal{M} and the development of efficient algorithms for the optimal leader selection under MSGs. In addition, the restrictions on our analysis can be relaxed, allowing for directed, weighted, and/or disconnected graphs.

REFERENCES

- [1] G. F. Young, L. Scardovi, and N. E. Leonard, "Robustness of noisy consensus dynamics with directed communication," in *American Control Conference*. IEEE, 2010, pp. 6312–6317.
- [2] D. Zelazo and M. Burger, "On the robustness of uncertain consensus networks," *IEEE Trans. Control Netw. Syst.*, 2015.
- [3] M. Siami and N. Motee, "Fundamental limits and tradeoffs on disturbance propagation in linear dynamical networks," *IEEE Trans. Autom. Control*, vol. 61, no. 12, pp. 4055–4062, 2016.
- [4] B. Bamieh, M. R. Jovanovic, P. Mitra, and S. Patterson, "Coherence in large-scale networks: Dimension-dependent limitations of local feedback," *IEEE Trans. Autom. Control*, vol. 57, no. 9, pp. 2235–2249, 2012.
- [5] L. Xiao, S. Boyd, and S.-J. Kim, "Distributed average consensus with least-mean-square deviation," *J Parallel Distrib Comput*, vol. 67, no. 1, pp. 33–46, 2007.
- [6] L. Moreau, "Stability of multiagent systems with time-dependent communication links," *IEEE Trans. Autom. Control*, vol. 50, no. 2, pp. 169–182, 2005.
- [7] R. Olfati-Saber, J. A. Fax, and R. M. Murray, "Consensus and cooperation in networked multi-agent systems," in *Proceedings of the IEEE*, vol. 95, no. 1. IEEE, 2007, pp. 215–233.
- [8] I. Matei, J. S. Baras, and C. Somarakis, "Convergence results for the linear consensus problem under Markovian random graphs," *SIAM J. Control Optim.*, vol. 51, no. 2, pp. 1574–1591, 2013.
- [9] A. Tahbaz-Salehi and A. Jadbabaie, "Consensus over ergodic stationary graph processes," *IEEE Trans. Autom. Control*, vol. 55, no. 1, pp. 225–230, 2010.
- [10] B. Touri and A. Nedic, "On ergodicity, infinite flow, and consensus in random models," *IEEE Trans. Autom. Control*, vol. 56, no. 7, pp. 1593–1605, 2011.
- [11] S. Patterson and B. Bamieh, "Leader selection for optimal network coherence," in *Proc. IEEE CDC*. IEEE, 2010, pp. 2692–2697.
- [12] F. Lin, M. Fardad, and M. R. Jovanovic, "Algorithms for leader selection in stochastically forced consensus networks," *IEEE Trans. Autom. Control*, vol. 59, no. 7, pp. 1789–1802, 2014.
- [13] K. Fitch and N. E. Leonard, "Joint centrality distinguishes optimal leaders in noisy networks," *IEEE Trans. Control Netw. Syst.*, vol. 3, no. 4, pp. 366–378, 2015.
- [14] A. Clark, L. Bushnell, and R. Poovendran, "A supermodular optimization framework for leader selection under link noise in linear multi-agent systems," *IEEE Trans. Autom. Control*, vol. 59, no. 2, pp. 283–296, 2014.
- [15] O. L. do Valle Costa, M. D. Fragoso, and M. G. Todorov, *Continuous-time Markov Jump Linear Systems*. Springer Science & Business Media, 2012.
- [16] V. Gupta, R. M. Murray, L. Shi, and B. Sinopoli, "Networked sensing, estimation and control systems," *CalTech Report*, 2009.
- [17] X. Feng, K. A. Loparo, Y. Ji, and H. J. Chizeck, "Stochastic stability properties of jump linear systems," *IEEE Trans. Autom. Control*, vol. 37, no. 1, pp. 38–53, 1992.
- [18] R. Agaev and P. Chebotarev, "On the spectra of nonsymmetric Laplacian matrices," *Linear Algebra and its Applications*, vol. 399, pp. 157–168, 2005.
- [19] G. F. Young, "Optimising robustness of consensus to noise on directed networks," Ph.D. dissertation, Princeton University, 2014.
- [20] P. Barooah and J. P. Hespanha, "Estimation from relative measurements: Electrical analogy and large graphs," *IEEE Trans. Signal Process.*, vol. 56, no. 6, pp. 2181–2193, 2008.
- [21] G. F. Young, L. Scardovi, and N. E. Leonard, "A new notion of effective resistance for directed graphs-part I: Definition and properties," *IEEE Trans. Autom. Control*, vol. 61, no. 7, pp. 1727–1736, 2016.
- [22] —, "A new notion of effective resistance for directed graphs-part II: Computing resistances," *IEEE Trans. Autom. Control*, vol. 61, no. 7, pp. 1737–1752, 2016.
- [23] —, "Rearranging trees for robust consensus," in *Proc. IEEE CDC-ECC*, 2011, pp. 1000–1005.
- [24] I. Poulakakis, G. F. Young, L. Scardovi, and N. E. Leonard, "Information centrality and ordering of nodes for accuracy in noisy decision-making networks," *IEEE Trans. Autom. Control*, vol. 61, no. 4, pp. 1040–1045, 2016.
- [25] V. Srivastava and N. E. Leonard, "Collective decision-making in ideal networks: The speed-accuracy trade-off," *IEEE Trans. Control Netw. Syst.*, vol. 1, no. 1, pp. 121–132, 2014.
- [26] K. Stephenson and M. Zelen, "Rethinking centrality: Methods and examples," *Social Networks*, vol. 11, no. 1, pp. 1–37, 1989.
- [27] S. Patterson, N. McGlohon, and K. Dyagilev, "Optimal k-leader selection for coherence and convergence rate in one-dimensional networks," *IEEE Trans. Control Netw. Syst.*, 2016.
- [28] M. Siami, S. Bolouki, B. Bamieh, and N. Motee, "Centrality measures in linear consensus networks with structured network uncertainties," *IEEE Trans. Control Netw. Syst.*, 2017.